Study of Effect on Resonance Frequency of Piezoelectric Unimorph Cantilever for Energy Harvesting

G. Ravi Prakash*, K. M. Vinayaka Swamy, S. Huddar, B. G. Sheeparamatti,
Department of Electronics and Communication Engineering
Basaveshwar Engineering College, Bagalkot-587102, Karnataka, India.
Corresponding author*:sgravi2@gmail.com

Abstract

The focus of this paper is to study the effect on resonance frequency and power enhancement techniques of piezoelectric MEMS. The modeling, design, and optimization of a piezoelectric generator based on a two-layer bending element using COMSOL Multiphysics. An analytical relation was developed based on the shift in resonance frequency caused by the addition of a thin film on the cantilever. The theoretical analysis is done with a user-friendly MATLAB/Simulink interface constructed for easy introduction of design dimensions , material parameter values and force signal stimuli. Power output is proportional to the proof mass attached to the system. Therefore, the proof mass should be maximized while maintaining other constraints such as resonance frequency and strain limits . Power output is inversely related to the driving and resonance frequency. Therefore, designing for lower frequency peaks in the vibration range is preferred as long as they have equivalent or higher acceleration magnitude than higher frequency peaks. Upon review of published piezoelectric microgenerators in this field, it is found that the proposed design of the piezoelectric energy harvester offers a best figure of merit (FOM) and promising output voltage.

Key words: Piezo-microcantilevers, Energy harvesting, micro-generators

1. Introduction

With recent growth in the development of low-power electronic devices such as microelectronics and wireless sensor nodes, as well as the global interest in the concept of "green" engineering, the topic of energy harvesting has received much attention in the past decade. The energy requirements of low-power electronics have steadily decreased with advancements in efficient circuitry such that energy harvesting systems can be considered feasible solutions in providing power to self-powered systems. Conventional low-power electronics, such as wireless sensor nodes, rely on batteries to provide power to the device. The use of batteries, however, presents several drawbacks including the cost of battery replacement as well as limitations imposed by the need of convenient access to the device for battery replacement purposes. By scavenging ambient energy surrounding an electronic device, energy harvesting solutions have the ability to provide permanent power sources that do not require periodic replacement. Such systems can operate in an autonomous, self-powered manner.

Piezoelectric thin films offer a number of advantages in MEMS applications due to their efficient voltage-deflection conversion, high energy densities, low noise, high frequency operation, and low power requirements. In MEMS technology, the most used piezoelectric thin films are pyroelectric AlN and ZnO (in their wurtzite structure) and ferroelectric PZT. The major difference between ferroelectric and pyroelectric is the possibility of reorienting the internal polarization upon application of an electric field: possible in ferroelectrics with fields above the material coercive field, it is absent in pyroelectrics

2. Theoretical Consideration

One can formulate a general model for the conversion of the kinetic energy of a vibrating mass to electrical power based on linear system theory without specifying the mechanism by which the conversion takes place. A simple model based on the schematic is shown in Figure 1**.** When the piezo generator structure is excited with a sinusoidal force around its resonance frequency, with small displacements where the movements remain linear, e.g. linear elastic, it can be modeled as a structure with: A rigid mass, M, spring, K, damper, (b_e , b_m) as shown in figure 1.

When the generator is vibrated by a vibratory movement, $y(t)$, the mass moves out of phase with

the generator housing, so that there is a net movement between the mass and the housing

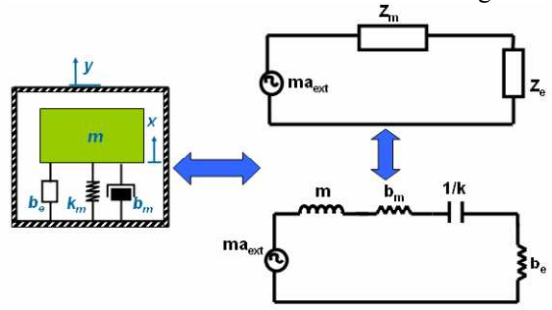

Figure 1 Schematic of a generic vibration energy harvester [1].

. This relative displacement, $z(t)$, is alternating and can drive a transducer to generate electric energy. The transducer is depicted as a dashpot, b_e, because the conversion of mechanical energy into electrical energy damps the mass. In addition, the mass can also be damped by mechanical damping, such as internal strain rate damping and external air damping. The mechanical damping is depicted as a second dashpot, b_m, in Figure 1 and equivalent electrical circuit shows the force-voltage analogue where mass m acts as inductor spring 1/k as capacitor and damping (b_e, b_m) as resistor .

The energy harvester can be formulated as second order differential equation [1-12] as

$$m\ddot{z}(t)+(b_e+b_m)\dot{z}(t)+kz(t)=-m\ddot{y}(t) \qquad (1)$$

The resonant frequency (fr) can be calculated by Equation 8[14]

$$f_r=\frac{\omega}{2\pi}=\frac{1}{2\pi}\sqrt{\frac{K}{m_e}} \qquad (2)$$

The equation 8 can be express in terms of bending modulus per unit width D_p by

$$f_n=\frac{v_n^2}{2\pi}\frac{1}{l^2}\sqrt{\frac{D_p}{m}} \qquad (3)$$

$$m=\rho_p t_p+\rho_s t_s \qquad (4)$$

Where the mass per unit area m is calculated by the thicknesses and densities, ρ_p and ρ_s are the densities of the PZT and substrate, respectively.

The bending modulus (D_p) is a function of Young's modulus and thickness and is expressed by

$$D_p=\frac{E_p^2t_p^2+E_s^2t_s^2+2E_pE_st_pt_s(2t_p^2+2t_s^2+3t_pt_s)}{12(E_pt_p+E_st_s)} \qquad (5)$$

Where E_p (ZnO) and E_s (Pt) are Young's modules of two materials and their thicknesses, t_p and t_s, on the tip of the cantilever.

For a traditional piezoelectric unimorph cantilever with a Piezo layer of the same length as the substrate layer as schematically shown in Figure 2. The quantities, such as induced voltage per unit force[3], $V_{in,ave/F}$, Spring constant K and the induced voltage per tip displacement $V_{in,ave/htip}$ is given by equations 6, 7 and 8

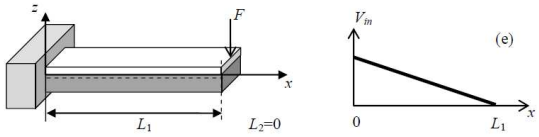

Figure 2. The schematic of a PUC with the NPL/PL length, and the corresponding induced voltage distribution in the piezoelectric layer with a concentrated force, F, applied at the tip.

$$\frac{V_{in.ave}}{F}=\frac{1}{2}Lg_{31}\frac{E_p}{wD_1}\left(t_{n1}t_p+\frac{1}{2}t_p^2\right) \qquad (6)$$

$$K=\frac{2wD}{L^3} \qquad (7)$$

$$\frac{V_{in.ave}}{h_{tip}}=\frac{3}{4}\frac{g_{31}E_st_sE_pt_p(t_s+t_p)}{L^2(E_st_s+E_pt_p)} \qquad (8)$$

Where L is the length of cantilever, g_{31} piezoelectric voltage constant ,t_{n1} is the position of neutral axis, t_p, t_s, E_p, E_s are the thickness and young's modules of piezo and substrate layer, w is the width, D is the bending modulus. The analytical simulation using Matlab Simulink as shown in Figure 3 includes calculation of Displacement, Voltage and material parameters.

For simplicity, only the voltage generation characteristics of the material are accounted for in Matlab/Simulink, Figure 3 shows the complete piezoelectric model as implemented in Matlab/Simulink.

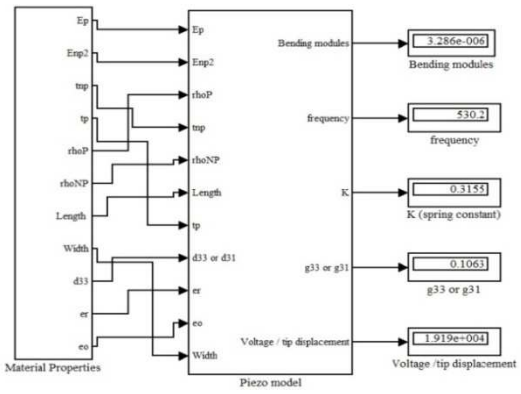

Figure 3. Simulink model of piezoelectric unimorph cantilever.

3. Geometric Modeling

3D geometry is considered for the simulations. The piezoelectric converter has a unimorph cantilever shape, as shown in Figure 4. The device is made by a platinum base with a piezoelectric layer ZnO on the top, poled along the thickness direction.

For d_{31} top Pt and Pt base will act as electrode however for d_{33} a ZnO is deposited over thin $SiO2$/Pt and for electrical contacts electrode are pattern in interdigitated form, Piezoelectric unimorph cantilever as dimensions 2500µm×500µm and substrate(Pt) layer as thickness 4µm and piezo layer(ZnO) as 2µm is shown in Figure 4**.**

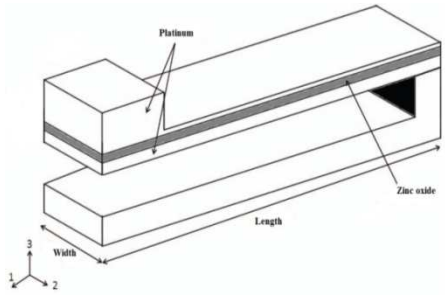

F**igure 4**. A unimorph piezoelectric generator cantilever showing the acceleration force applied in Z-direction.

4. Modeling using COMSOL Multiphysics

The Body load F (Acceleration× density) is given as input to piezoelectric layer to induce a strain

The model uses a piezoelectric application mode for the simulation of the mechanical and the electrical behavior of the converter when a sinusoidal vertical acceleration is applied. The moving mesh application mode was used for changing the thickness of the piezoelectric layer, computing the mesh deformation with the arbitrary Lagrangian Eulerian (ALE) technique.

4.1 Meshing

The mesh is composed of 432 quad elements for a total number of degrees of freedom of 6076. The mesh is created using the mapped mesh tool dividing the length of the converter into 20 elements exponentially spaced with an element ratio equal to 10, with a finer mesh near the clamped end. Each material layer is divided in 2 linearly spaced elements along the thickness, and in 4 linearly spaced elements along width. A swept mesh is done using opposite vertical surfaces of each layer as source face and target face. Figure 5 shows the obtained mesh.

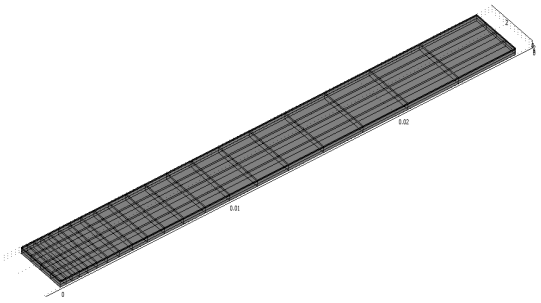

Figure 5. piezoelectric converter meshes.

4.2 Subdomain Settings

The Structure is composed into two subdomains that is base layer, piezoelectric layer. Platinum is chosen as the base because of its high young modulus value of 168 x 10^9 Pa and high density ρ value of 21450Kg/m^3. Taking fabrication of device into account ZnO is used as piezo ceramic material having following characteristics.

Elastic Compliance matrix

$$s^E = \begin{bmatrix} 7.9 & -3.4 & -2.2 & 0 & 0 & 0 \\ -3.4 & 7.9 & -2.2 & 0 & 0 & 0 \\ -2.2 & -2.2 & 6.9 & 0 & 0 & 0 \\ 0 & 0 & 0 & 24 & 0 & 0 \\ 0 & 0 & 0 & 0 & 24 & 0 \\ 0 & 0 & 0 & 0 & 0 & 23 \end{bmatrix} \times 10^{-12} Pa^{-1}$$

Coupling matrix

$$d = \begin{bmatrix} 0 & 0 & 0 & 0 & -11 & 0 \\ 0 & 0 & 0 & -11 & 0 & 0 \\ -5.4 & -5.4 & 12 & 0 & 0 & 0 \end{bmatrix} \times 10^{-12} CN^{-1}$$

Relative permittivity matrix

$$\varepsilon_r = \begin{bmatrix} 9.16 & 0 & 0 \\ 0 & 9.16 & 0 \\ 0 & 0 & 12.64 \end{bmatrix}$$

Density

$$\rho = 5680 Kg / m^3$$

An acceleration of 1 g is applied in each subdomain, which results in $force/volume = \rho.a$ where ρ is the density of ZnO and a is the acceleration constant.

4.3 Boundary Settings

One cantilever end is fixed while other is free for vibration. Therefore the fixed constraint condition is applied for the vertical faces of both the layers, while all the other faces are free for displacement. In order to pole piezoelectric layer in direction 3, the electrical behavior of the ZnO must be considered and it is modeled with the electrostatic boundary conditions. d_{31} mode is selected by making floating potential for the upper face and grounding lower face of the ZnO layer and for d_{33} clamp vertical face and freely suspended vertical face are selected as floating and ground potential respectively, while all other faces of the piezoelectric layer are kept as zero charge/Symmetry constraint.

4.4 Moving Mesh

A moving mesh is used in order to change the thickness, length and width of both the piezoelectric layer (ZnO) and Platinum base. The bottom face of the piezoelectric subdomain is constrained as a clamp while the vertical faces are clamped along normal direction and left unconstrained along tangential direction allowing it to stretch freely. The upper face of the piezoelectric layer is tangentially constrained and displaced in direction normal to the surface. The displacement is incremented using three parameter delta thick, delta length and delta width.

4.5 Simulation Results

Model Frequency Analysis

Because the fundamental resonance mode is the mode of bending, the bending resonance frequencies and the relevant mode shapes were modeled. The results related to the first six frequencies as shown in figure 6.

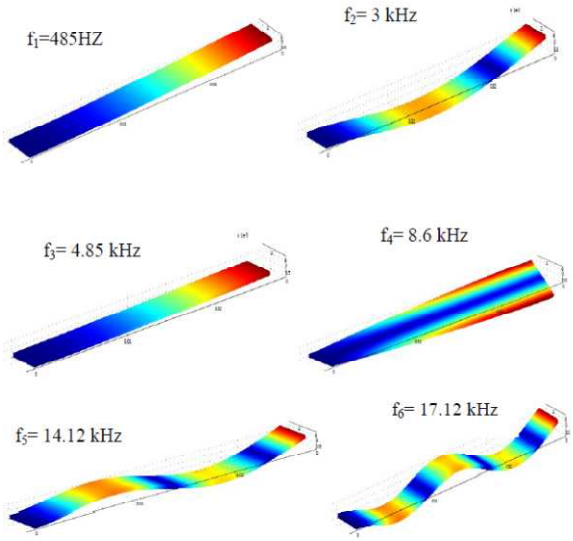

Figure 6. .Model frequency of piezoelectric unimorph cantilever.

Frequency Analysis

Frequency analysis is carried out in order to obtain the maximum voltage at resonance, frequency from 430Hz to 530Hz is varied, The resonant frequency for both d_{31} and d_{33} structure is 485 Hz as shown in Figure 7 and Figure 8.

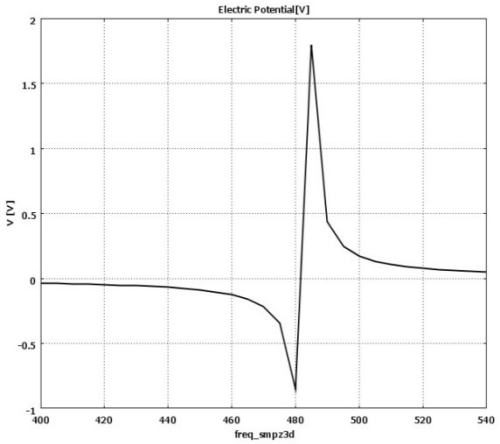

Figure 7. Frequency Response of $d31$

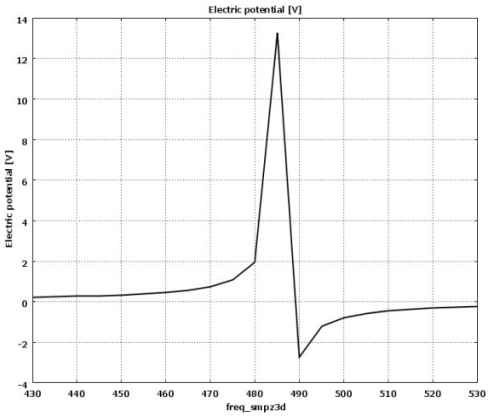

Figure 8. Frequency Response of $d33$

Static analysis

For an applied load of 1g the static displacement and voltage generated for d_{31} and d_{33} is shown in the figure 9.

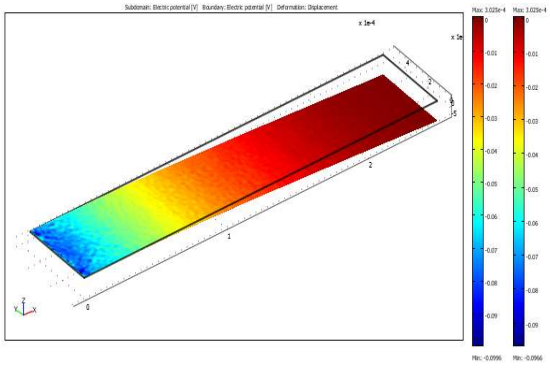

Figure 9. Microcantilever showing voltage developed due to applied acceleration of 1g**.**

Transient Analysis

In transient response analysis force per unit area is taken as 50 N/m^2, which is equivalent to a proof mass of 0.145 mg deposited on tip of cantilever at 9.81m/s^2 acceleration. This mass is obtained from the following equations,

$$Fz = Mass.Acceleration.Area$$

Where F_z is force per unit area,

$$Area = 120\mu m.\,(blocklength)\,,$$

$$Density = Mass/Volume$$

Platinum is chosen for its high density value of $\rho = 21450 Kg/m^3$

Damping is very important in the transient analysis in order to get results that are close to the reality. The model uses Rayleigh damping for transient analysis. This damping is represented by the following equation:

$$c = \alpha M + \beta K \qquad (9)$$

Where C is the damping matrix, M is the mass matrix and K is the stiffness matrix. In order to find the damping coefficients α and β, the relationship between the critical damping ratio and the Rayleigh damping is used. These parameters are given by:

$$\begin{bmatrix} \frac{1}{2\omega_1} & \frac{\omega_1}{2} \\ \frac{1}{\omega_2} & \frac{\omega_2}{2} \end{bmatrix} \begin{bmatrix} \alpha \\ \beta \end{bmatrix} = \begin{bmatrix} \xi_1 \\ \xi_2 \end{bmatrix} \qquad (10)$$

Where ζ is the critical damping ratio at a specific angular velocity ω. By using corresponding ζ and ω pair, one can compute the damping parameters α and β. These calculations are carried out by the solving eq (10) where ω_1 and ω_2 are kept 450 Hz and 510 Hz respectively which are near to excitation frequency of 485Hz. Both the damping ratios ζ_1 and ζ_2 is taken as 0.1,on substituting we get α=49.5 and $\beta = 1.98\times10^{-4}$.

In order to get maximum peak to peak voltage transient analysis is carried out at 485Hz. Changing position of electrode as describe earlier 2.1V and 8.2V are obtained for $d31$ and $d33$ respectively as shown in Figure 10 and Figure 11. By carrying out a static analysis with a particular force applied, one can find the maximum displacement along the beam length and the same is shown in Figure 12. From this graph the

minimum separation length between Pt base and substrate can be obtained.

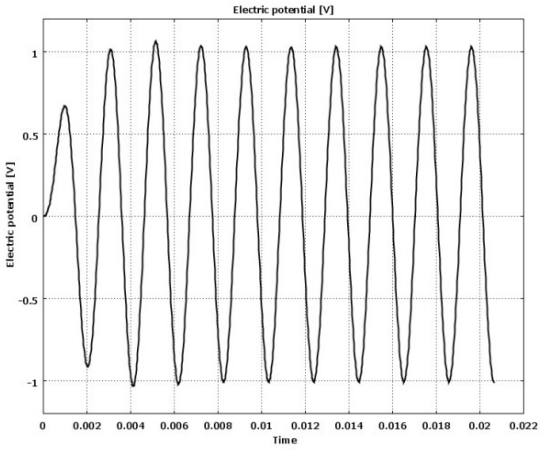

Figure 10. Transient Response of $d31$

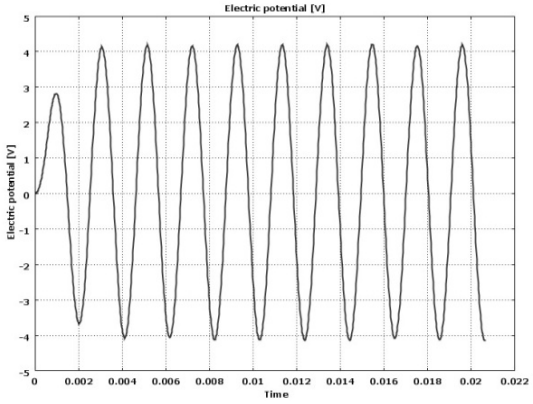

Figure 11 Transient Response of d_{33}

Parametric Segregated Analysis

In order to find optimized dimension for energy harvester, microscale dimensions are varied to produce maximum voltage using moving mesh ALE method. The length of ZnO and Pt base is varied from -400e-6 to 2500e-6 respectively by keeping initial length as 500e-6 and voltage versus length graph is plotted as shown in Figure 13. From figure maximum voltage is observing at lengt1h of 400e-6m and the figure 16 shows maximum displacement observed at length of 400e-6m, hence when cantilever have maximum displacement it generates a maximum voltage which is observed in figures 15 & 16.

Figure 12 shows extrusion plot showing electric potential .

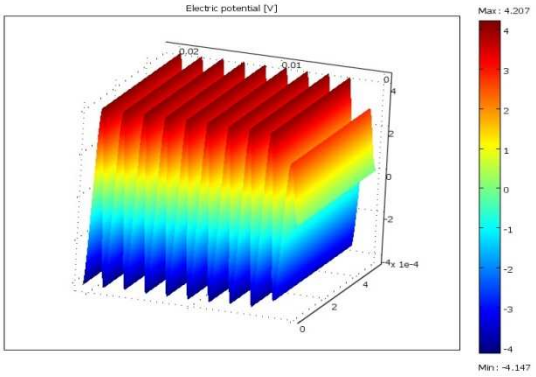

Figure 12 Extrusion plot showing total displacement of d_{33}

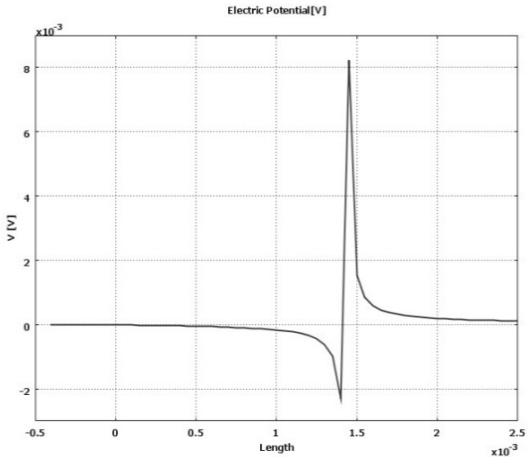

Figure 13 Extrusion plot showing total displacement of d_{33}

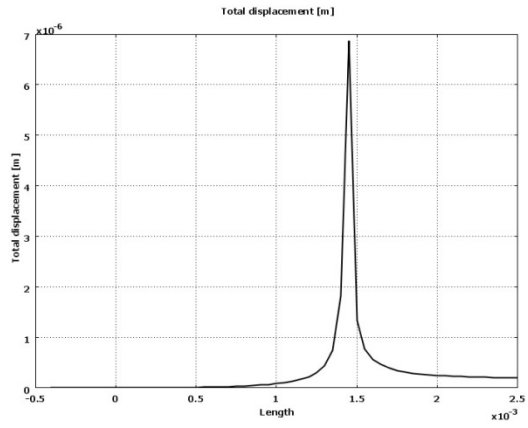

Figure 14 Plot of total displacement vs length

Figure 15shows extrusion plot shows maximum voltage observing at length of 1500e-6m.

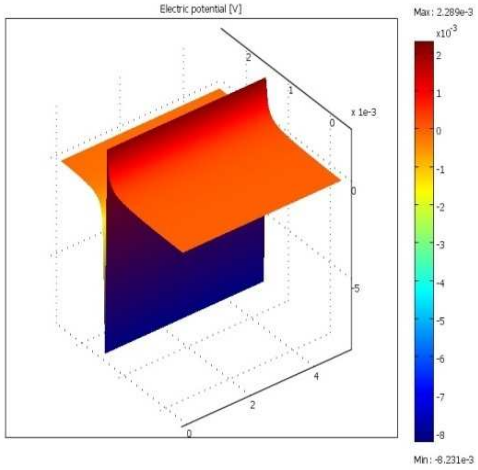

Figure 15 extrusion plot for maximum voltage.

Figure 16 shows extrusion plot shows maximum displacement at length of 1500e-6m.

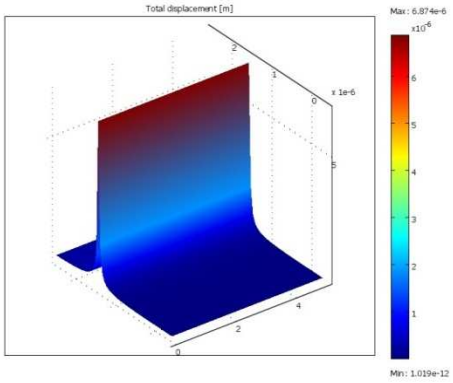

Figure 16 Extrusion plot for maximum displacement.

Figure of Merit (FOM)

A FOM based on voltage generated per unit volume per acceleration is used to compare the performances of different energy harvesters in Table 1. For the optimized structure proposed in this work a FOM value for $d31$ is 420 $V/mm3.g$ and while that of $d33$ is 1680 $V/mm^3.g$. This FOM is higher than other works reported for $d31$ and $d33$ modes implementations. The proposed structure offers a best Figure of merit when compared to other works and promising output voltage.

5. Conclusion

An energy harvester based on piezoelectric micro generator is designed and simulated in COMSOL MultiPhysics. The structure design and optimization were carried out for both piezo-ceramic and platinum base dimensions. The thickness, length and width of metal base and ZnO were varied in order to get maximum displacement and voltage. A composite cantilever with dimensions 2500 μm x 500 μm x 6 μm is used to harvest vibration energy. A proof mass of 0.145 mg is placed on tip of cantilever to lower the resonance frequency and to maximize the output voltage. Cantilever beam is operated at a resonance frequency of 485 Hz, 1 g acceleration and the output voltage obtained is 2.1V for d_{31} and 8.5 V for d_{33}. Compared to reported microgenerators the proposed device offers good Figure of merit and promising output voltage.

Table .1 Performance Comparisons with reported MEMS harvesters

Ref	Device	Dimension	V_{peak}	F(Hz)	FOM V/mm^3g
[13]	$d31$ PZT	2mm X 0.6mm X 1.64μm	0.45	608	228.7
[14]	$d31$ PZT	2mmX3.2mmX 1.39μm	16	60	142.3
[15]	$d31$ ZnO	27mm x .3mm x 0.2mm.	4.7×10^{-9}	10	$.9\times10^{-9}$
[16]	$d33$ PZT	0.8mmX1mmX 10μm	2.2	528	705
[17]	$d33$ PZT	0.8mmX1.2mm X2μm	1.6	870	416.6
Proposed	**$d31$ ZnO**	**2.5mm x .5mm x 2μm.**	**1.05**	**485**	**420**
Proposed	**$d33$ ZnO**	**2.5mm x .5mm x 2μm**	**4.2**	**485**	**1680**

References

1] S. Roundy, P.K. Wright, J. Rabaey, A study of low level vibrations as a power source for wireless sensor nodes, Comput. Commun. 2 (2003) 1131–1144.

[2] A. Chandrakasan, R. Amirtharajah, J. Goodman, W. Rabiner, Trends in low power

digital signal processing, in: Proceedings of the 1998 IEEE International Symposium on Circuits and Systems, ISCAS'98, 1998.

[3] S. Meninger, J.O. Mur-Miranda, R. Amirtharajah, A.P. Chandrakasan, Vibration to electric energy conversion, IEEE Transact. VLSI Syst. 9 (2001) 64–76.

[4] W.R. Davis, N. Zhang, K. Camera, F. Chen, D. Markovic, N. Chan, B. Nikolic, R. Brodersen, A design environment for high throughput, low power dedicated signal processing systemsdkjdot, in: Proceedings of the IEEE Custom Integrated Circuits Conference, San Diego, CA, USA, 2001.

[5] C.W. Wong, Y. Jeon, G. Barbastathis, S.-G. Kim, Strain-tuning of periodic optical devices: tunable gratings and photonic crystals, Technical Digest of the 2002 Solid-State Sensor and Actuator Workshop, Hilton Head Island, SC, 2002, pp. 342–345.

[6] K. Hwang, M. Koo, S. Kim, High-brightness projection display systems based on the thin-film actuated mirror array (TFAMA), in: Proceedings of SPIE, Santa Clara, CA, USA, September 1998, pp. 171–180.

[7] P. Glynne-Jones, S.P. Beeby, N.M. White, Towards a piezoelectric vibration-powered microgenerator, IEE Proc. Sci., Meas. Technol. 148 (2001) 69–72.

[8] J. Kymissis, C. Kendall, J. Paradiso, N. Gershenfeld, Parasitic power harvesting in shoes, in: Proceedings of the Second IEEE International Conference on Wearable Computing ISWC, Pittsburgh, PA, USA, 1998.

[9] B. Xu, Y. Ye, L.E. Cross, J. Bernstein, R. Miller, Dielectric hysteresis from transverse electric fields in lead zirconate titanate thin films, Appl. Phys. Lett. 74 (1999) 3549–3551.

[10] J.J. Bernstein, J. Bottari, K. Houston, G. Kirkos, R. Miller, B. Xu, Y. Ye, L.E. Cross, Advanced MEMS ferroelectric ultrasound 2D arrays, in: IEEE 1999 Ultrasonics Symposium, Lake Tahoe, NV, 1999.

[11] R. Sood, Y.B. Jeon, J.H. Jeong, S.G. Kim, Piezoelectric micro power generator for energy harvesting, Technical Digest of the 2004 Solid- State Sensor and Actuator Workshop, Hilton Head, South Carolina, 2004.

[12] C.B. Williams, R.B. Yates, Analysis of a micro electric generator for microsystems, Sens. Actuators 52 (1996) 8–11.

[13] Hua Bin Fanga, Jing Quan Liua, Zheng Yi Xub, Lu Donga, Li Wangb, Di Chena, Bing-Chu Caia, Yue Liub, "Fabrication and performance of MEMS-based piezoelectric power generator for vibration energy harvesting," *Microelectronics Journal*, vol. 37, pp. 1280 – 1284, July 2006.

[14] Wen G. Li, Siyuan He and Shudong Yu, "Improving power density of a cantilever piezoelectric power harvester through a curved L-shaped proof mass," *IEEE Transactions On Industrial Electronics*, vol. 57, pp. 868 – 876, March 2010.

[15] M. Guizzetti, V. Ferrari, D. Marioli and T. Zawada, "Thickness optimization of a piezoelectric converter for energy harvesting," *Proceedings of*

[16] J.C. Park, D. H. Lee, J. Y. Park, Y. S. Chang and Y. P. Lee, "High performance piezoelectric MEMS energy harvester based on d_{33} mode of PZT thin film on buffer-layer with $PbTiO_3$ inter-layer," *IEEE Solid-State Sensors, Actuators and Microsystems Conference*, pp. 517 – 520,June 2009.

[17] P. Muralta, M. Marzenckib, B. Belgacema, F. Calamea and S. Basrourb, "Vibration energy harvesting with PZT micro device," *Elsevier Proceedings of the Eurosensors XXIII conference*, pp. 1194–1196, 2009.